JAST (Journal of Animal Science and Technology) TITLE PAGE

Upload this completed form to website with submission

ARTICLE INFORMATION	Fill in information in each box below
Article Type	Research article
Article Title (within 20 words without abbreviations)	Characterization of sustainable bacterial cellulose of *Komagataeibacter rhaeticus* SLAM-JS1B isolated from Kombucha for biocontrol of Salmonella Typhimurium in animal production system
Running Title (within 10 words)	Antimicrobial property of BC of *K. rhaeticus* from Kombucha
Author	Jiseong Mun, Min-Geun Kang, Junhyeok Kyung, Youbin Choi, Sangdon Ryu, Jongnam Kim, and Younghoon Kim
Affiliation	1Department of Agricultural Biotechnology and Research Institute of Agriculture and Life Science, Seoul National University, Seoul 08826, Korea 2Honam National Institute of Biological Resources, Mokpo 58762, Korea 3Department of Food Science & Nutrition, Dongseo University, Busan 47011, Korea
ORCID (for more information, please visit https://orcid.org)	Jiseong Mun (https://orcid.org/0009-0004-7983-8283) Min-Geun Kang (https://orcid.org/0000-0002-2204-6443) Junhyeok Kyung (https://orcid.org/0009-0004-3596-6769) Youbin Choi (https://orcid.org/0000-0002-9444-3237) Sangdon Ryu (https://orcid.org/0000-0001-5338-8385) Jongnam Kim (https://orcid.org/0000-0002-8034-7156) Younghoon Kim (https://orcid.org/0000-0001-6769-0657)
Competing Interests	No potential conflict of interest relevant to this article was reported.
Funding Sources State funding sources (grants, funding sources, equipment, and supplies). Include name and number of grant if available.	This project was supported in part by grants from a National Research Foundation of Korea Grant, funded by the Korean government (MEST; 2021R1A2C3011051) and by the support of "Cooperative Research Program for Agriculture Science and Technology Development (Project No. RS-2025-02263976)" Rural Development Administration, Republic of Korea.
Acknowledgments	
Availability Of Data And Material	Upon reasonable request, the datasets for this study can be obtained from the corresponding author.
Authors' Contributions Please specify the authors' role using this form.	Conceptualization: Mun J, Kang MG, Kim Y. Data curation: Mun J, Kang MG. Formal analysis: Mun J, Kang MG. Methodology: Mun J, Kang MG. Software: Mun J, Kang MG. Validation: Mun J, Kang MG, Kyung J, Choi Y, Kim J, Kim Y. Investigation: Mun J, Kang MG. Writing - original draft: Mun J, Kang MG, Kyung J, Choi Y, Kim J, Kim Y. Writing - review and editing: Mun J, Kang MG, Kyung J, Choi Y, Kim J, Kim Y.
Ethics Approval And Consent To Participate	This study does not require IRB/IACUC approval because there are no human and animal participants.

CORRESPONDING AUTHOR CONTACT INFORMATION

For the corresponding author (responsible for correspondence, proofreading, and reprints)	Fill in information in each box below
First name, middle initial, last name	Younghoon Kim
Email address—this is where your proofs will be sent	ykeys2584@snu.ac.kr
Secondary Email address	
Address	Department of Agricultural Biotechnology and Research Institute of Agriculture and Life Science, Seoul National University, Seoul 08826, Korea
Cell phone number	+82-10-4135-2584
Office phone number	+82-02-880-4808
Fax number	+82-02-873-2271

Characterization of sustainable bacterial cellulose of *Komagataeibacter rhaeticus* SLAM-JS1B isolated from Kombucha for biocontrol of *Salmonella* Typhimurium in animal production system

Jiseong Mun[a,†], Min-Geun Kang[a,†], Junhyeok Kyung[a], Youbin Choi[a], Sangdon Ryu[b], Jongnam Kim[c], and Younghoon Kim[a,*]

[a]Department of Agricultural Biotechnology and Research Institute of Agriculture and Life Science, Seoul National University, Seoul 08826, Korea

[b]Honam National Institute of Biological Resources, Mokpo 58762, Korea

[c]Department of Food Science & Nutrition, Dongseo University, Busan 47011, Korea

†These authors contributed equally to this work.

*To whom correspondence should be addressed: ykeys2584@snu.ac.kr

Abstract

Bacterial cellulose (BC) is a high-purity, nanofibrillar biomaterial with considerable potential in the animal industry as both a functional dietary fiber and a carrier for bioactive compounds. In this study, three BC-producing *Komagataeibacter* strains were isolated from kombucha pellicles (*K. intermedius* SLAM-NK6B, *K. rhaeticus* SLAM-JS1B, and *K. rhaeticus* SLAM-JS2B), and their cellulose production under static conditions at 25°C was compared. The *K. rhaeticus* strains formed substantially thicker pellicles than *K. intermedius* with dry weight yields of 120.8 ± 28.3 mg/L (SLAM-JS1B), 113.3 ± 15.0 mg/L (SLAM-JS2B), and 36.3 ± 5.3 mg/L (SLAM-NK6B), respectively. Leveraging the highest-yielding strain SLAM-JS1B, a sequential optimization strategy including one-variable-at-a-time (OVAT) screening, Plackett–Burman design (PBD), and Box–Behnken design (BBD) combined with response surface methodology, was employed to enhance BC production. Yeast extract, $MgSO_4$, and ethanol were identified as key drivers. The optimized medium (10 g/L yeast extract, 2 g/L $MgSO_4$, 10 mL/L ethanol, with glucose and KH_2PO_4 maintained within the design-space ranges) yielded a cellulose titer of 2.795 g/L, representing a 37% increase relative to the baseline Saleh medium. Characterization by FT-IR and FE-SEM confirmed the structural, chemical, and morphological characteristics of BC, revealing a dense, highly porous nanofibrillar network. Furthermore, *Salmonella* Typhimurium–targeting phages were successfully immobilized on the BC matrix and retained lytic activity in antimicrobial assays. Collectively, our findings propose an optimized production platform for BC using *K. rhaeticus* SLAM-JS1B isolated from kombucha and highlight the functional utility of BC as a carrier for bioactives, underscoring its promise for pathogen biocontrol in animal production systems.

Keywords: *Komagataeibacter*, bacterial cellulose, nanofibrillar biomaterial, optimization production strategy, phage immobilization

Introduction

Cellulose is one of the most abundant polysaccharides on Earth, produced by a diverse array of organisms including plants and microorganisms [1, 2]. Although plants serve as the primary natural source of cellulose in nature, its industrial extraction and purification are often complicated by the co-existence of lignin and hemicellulose, necessitating intensive chemical treatments such as alkaline pulping, acid hydrolysis, and bleaching [3]. In contrast, bacterial cellulose (BC) is synthesized extracellularly in a nanofibrillar form, inherently free of lignin and hemicellulose, and thus requires minimal downstream processing [4]. Owing to the absence of recalcitrant components, BC shows strong potential as an alternative fibrous feed source for herbivores, including ruminants [5-8]. In addition to its purity, BC exhibits a suite of advantageous physicochemical properties, including nanoscale fibrillar architecture, exceptional mechanical strength, high crystallinity, and remarkable water-holding capacity [9]. By coupling its nanoscale architecture with superior biocompatibility, BC functions as an effective carrier for hydrophilic compounds and a suitable vehicle for targeted antimicrobial delivery in animal health applications. In this context, BC-based antimicrobial delivery strategies show great potential against representative feedborne pathogens of major economic concern in livestock industries, such as *Salmonella enterica* serovar Typhimurium *(S.* Typhimurium) [14-16]. Despite its considerable potential, however, the inherently low yield and slow productivity of BC represent significant barriers to its commercial feasibility [17]. These limitations underscore the need for advanced bioprocess optimization strategies to improve production efficiency and support the scalable application of BC across diverse industries.

The genus *Komagataeibacter* is widely recognized as one of the most prominent bacterial producers of cellulose, with numerous strains reported to achieve high yield capabilities [18]. The composition of the culture medium, particularly the types of carbon and nitrogen sources, directly affects microbial metabolism and the biosynthetic pathways involved in BC production [19]. Although most *Komagataeibacter* species require substantial nitrogen supplementation to achieve efficient cellulose biosynthesis, *K. rhaeticus* has recently garnered attention as a promising producer due to its capacity to maintain relatively high BC yields

even under nitrogen-limited conditions [20, 21]. The Hestrin–Schramm (HS) medium, one of the most widely used formulations for BC production, contains glucose (20 g/L) as the carbon source and peptone (5 g/L) together with yeast extract (5 g/L) as nitrogen sources [22, 23]. Notably, significant cost differences among these components have been reported, with glucose priced at approximately $0.70/kg, yeast extract at $1.70/kg, and peptone at $6.17/kg [24]. Consequently, nitrogen sources are a major cost driver in bacterial culture media for large-scale BC production. The intrinsic ability of *K. rhaeticus* to sustain high BC yields under reduced nitrogen input therefore confers a notable economic advantage. [20]. Although *K. rhaeticus* represents significant industrial potential, studies on the optimization of its BC production are still limited. A systematic investigation of strain-specific factors, including nutrient composition, additive supplementation, and physicochemical cultivation conditions, is essential to fully harness its potential as an efficient biocatalyst for BC synthesis.

In recent years, medium optimization for the production of microbially derived biomaterials has advanced markedly with the adoption of statistical methodologies, enhancing process efficiency, shortening experimental timelines, and reducing labor costs, thereby improving overall process economics. Strategic implementation of design-of-experiments approaches can substantially reduce the number of trials required for robust process optimization. For instance, a one-variable-at-a-time (OVAT) method was employed to investigate essential nutrient factors in the culture medium [25, 26]. The Plackett–Burman design (PBD) has proven highly effective for the preliminary screening of medium components, enabling the identification of significant variables with a minimal number of experimental runs [27]. While PBD is widely adopted for the initial optimization steps in fermentation processes, its limitation lies in the inability to evaluate interaction effects among variables. To address this limitation, the Box–Behnken design (BBD) offers a powerful follow-up approach, enabling the exploration of variable interactions and the development of predictive mathematical models for microbial productivity [28, 29].

In this study, we isolated *K. rhaeticus* SLAM-JS1B, a high-yielding BC-producing strain, from kombucha pellicles. Then, a three-step empirical, sequential statistical approach, including OVAT (for initial screening of nutrient preferences), PBD (for identifying key medium components), and BBD (for

analyzing interactions and defining optimal conditions), was employed to systematically optimize BC production. This sequential optimization framework significantly enhanced BC yield, improved process reproducibility, and enabled scalability for industrial application. Moreover, optimized cultivation of *K. rhaeticus* SLAM-JS1B yielded BC with characteristic nanofibrillar architecture, high water-holding capacity, and robust mechanical strength. These structural and physicochemical features also facilitated the effective immobilization of phages, supporting their potential utility as a bioactive delivery matrix [30]. Collectively, this work highlights the dual advantage of *K. rhaeticus*-derived BC as both a cost-effective biomaterial and a versatile platform for functional delivery applications in the animal industry.

Materials and methods

Isolation of bacterial cellulose (BC) producing strain

A kombucha starter culture maintained in our laboratory (Seoul National University, Seoul, South Korea) was used to isolate BC-producing strains. The starter was prepared by infusing green tea (Dongsuh, South Korea) into an 8% (w/v) cane sugar solution (United Farmer & Industry, Thailand) for 10 min, followed by sterilization by autoclaving, as described previously [31]. The culture was incubated under static, aerobic conditions at 25 °C for 20 days. Following incubation, the cellulose pellicle formed at the air–liquid interface was harvested and homogenized by blending it with an equal volume of 0.85% (w/v) saline using a commercial blender (HR3757, Philips, Netherlands). The resulting suspension was serially diluted and plated on MRS agar to isolate BC-producing strains. Using this procedure, *Komagataeibacter intermedius* SLAM-NK6B, *K. rhaeticus* SLAM-JS1B, and *K. rhaeticus* SLAM-JS2B were isolated [31]. Whole-genome sequencing of the isolates was performed, and the complete genome sequences have been deposited in GenBank under the following accession numbers: *K. intermedius* SLAM-NK6B (CP185240.1) and *K. rhaeticus* SLAM-JS1B (CP186559.1). The 16S rRNA gene sequence of *K. rhaeticus* SLAM-JS2B has also been deposited under the accession number (PX485042). Genomic analysis followed a previously established pipeline [32-35]. Long-read sequencing was conducted on the Oxford Nanopore MinION Mk1B platform (R10). The resulting reads were assessed using NanoPlot (v1.42.0), yielding 285,680 reads (mean read length, 9,327 bp; mean read quality, 18.5) and totaling 2,664,573,670 bp (~2.66 Gb). Assembly of the Nanopore reads resulted in a complete genome of 2,569,831 bp and a GC content of 62.85%. Annotation using the NCBI Prokaryotic Genome Annotation Pipeline predicted 2,520 protein-coding genes, 9 rRNA operons, and 58 tRNA genes. Orthologous Average Nucleotide Identity analysis showed the highest identity (99.48%) to the type strain, *K. rhaeticus* LMG 22126 [36].

Preparation of BC

BC was produced using *K. rhaeticus* SLAM-JS1B, previously isolated from kombucha pellicles. All reagents were purchased from Sigma-Aldrich (St. Louis, MO, USA) unless otherwise stated. The isolated strain was stored at −80 °C and subsequently cultured on modified Yamanaka medium containing 1.5% (w/v) D-glucose, 1.5% (w/v) yeast extract, 0.1% (w/v) KH_2PO_4, 0.1% (w/v) $MgSO_4$, 7 mL/L ethanol, and 1.5% (w/v) agar (pH 7.2) [4]. Plates were incubated at 25 °C for 3 days. A single colony was selected and inoculated into 3 mL of Yamanaka liquid medium in round-bottom test tubes (Falcon, Corning), then incubated at 25 °C for 3 days. Subsequently, 2 mL of the culture supernatant was transferred into 100 mL of Yamanaka liquid medium and incubated statically at 25 °C for 14 days.

After incubation, the BC pellicle was separated from the culture broth. The culture supernatant was filtered through a 0.2-μm pore-size polyvinylidene fluoride (PVDF) syringe filter (Whatman, Maidstone, UK) and stored at 4 °C until use. The harvested BC pellicles were treated with 0.5% NaOH at 90 °C for 30 min to remove bacterial cells and residual impurities, followed by repeated washing with distilled water (dH_2O) until neutral pH was reached [37]. The purified BC was freeze-dried to constant weight using a freeze dryer (Operon, Gyeonggi, South Korea). The final BC concentration was determined gravimetrically and expressed as grams per liter (g/L).

Optimization of BC production

One Variable at a Time (OVAT) Screening

To identify the most suitable basal medium for BC production by *K. rhaeticus* SLAM-JS1B, several standard BC media were first evaluated: Hestrin–Schramm medium (HS), modified HS medium (mHS), modified Yamanaka medium (MYM), modified glucose–yeast extract medium (GYM), and Saleh medium (SM) [4, 38-40]. The medium that supported the highest BC yield was selected as the basal medium for subsequent experiments. To assess the effects of different carbon and nitrogen sources on BC production, the OVAT method was employed. Various carbon sources, including glucose, sucrose, lactose, glycerol, sorbitol, and mannitol, were tested in the basal medium at a concentration of 1.5% (w/v). In parallel, several organic and inorganic nitrogen sources were evaluated in the basal medium at 1.3% (w/v), including yeast

extract, peptone, tryptone, ammonium nitrate, ammonium chloride, and ammonium sulfate. All fermentation experiments were carried out in 250 mL Erlenmeyer flasks containing 100 mL of sterile basal production medium. Cultures were incubated under static conditions at the specified temperature. Each condition was tested in triplicate to ensure reproducibility and statistical reliability of the results.

Plackett–Burman Design (PBD)

PBD was employed to evaluate the influence of various nutritional and physical parameters on BC production [27]. In this study, six independent variables were evaluated: glucose (X_1), yeast extract (X_2), KH_2PO_4 (X_3), $MgSO_4$ (X_4), ethanol (X_5), and incubation time (X_6). These variables were assessed across 12 experimental runs based on the PBD matrix, along with two additional center-point replicates to validate the model's accuracy. All experiments were conducted in triplicate to ensure statistical reliability. Each factor was tested at two levels, coded as +1 (high) and −1 (low). BC production (g/L) was used as the response variable. Table 1 summarizes the experimental design: each row represents an individual trial, and each column corresponds to a specific factor.

The experimental results were fitted to a first-order polynomial model, as shown in Equation (1):

$$Y = \beta_0 + \sum \beta_i X_i$$

where Y denotes the predicted BC production (g/L), β_0 is the model intercept, β_i is the estimated coefficient for each independent variable, and X_i is the coded level of the respective factor.

The statistical significance of each factor was assessed using regression analysis, including p-value calculations to evaluate each parameter's contribution to BC yield. All fermentation experiments were conducted in 250-mL Erlenmeyer flasks containing 100 mL of the respective media, formulated according to the PBD matrix.

Box-Behnken Design (BBD)

The most significant variables identified from the PBD were further optimized using a three-level BBD to determine the optimal conditions for maximum BC production [28, 29]. The application of BBD involved three primary steps: conducting statistically designed experiments, analyzing the experimental outcomes to model the predicted response, and validating the adequacy of the developed model.

Thirteen BBD runs were performed according to the design matrix, together with two center-point replicates (15 runs in total), to evaluate both the individual and interaction effects of the three key variables identified through PBD. These variables were yeast extract (X_1), $MgSO_4$ (X_2), and ethanol (X_3). Each factor was tested at three coded levels: −1 (low), 0 (center), and +1 (high), with 0 representing the mid-point of each experimental range (Table 2). All other medium components and cultivation parameters were maintained at their previously determined effective levels, classified as either high or low according to the regression analysis of the PBD results. A second-order (quadratic) polynomial model was employed to predict BC yield (Y) based on the interactions among the independent variables (X_1, X_2, and X_3).

The general form of the model is presented in Equation (2):

$$Y = \beta_0 + \beta_1X_1 + \beta_2X_2 + \beta_3X_3 + \beta_{12}X_1X_2 + \beta_{13}X_1X_3 + \beta_{23}X_2X_3 + \beta_{11}X_1^2 + \beta_{22}X_2^2 + \beta_{33}X_3^2$$

where Y is the predicted response (BC yield, g/L); β_0 is the intercept, β_1, β_2, and β_3 are the linear coefficients; β_{12}, β_{13}, and β_{23} are the interaction coefficients; and β_{11}, β_{22}, and β_{33} are the quadratic coefficients. The optimal values of the independent variables were estimated by taking the partial derivatives of the polynomial equation and setting them to zero. All experimental trials were conducted in triplicate to ensure reproducibility and statistical reliability.

Structural and physicochemical analysis of BC by Fourier-transform infrared (FT-IR) spectroscopy

Freeze-dried BC samples were analyzed by FT-IR spectroscopy and compared with a standard cellulose reference. Spectra were acquired with a Nicolet 6700 FT-IR spectrometer (Thermo Fisher Scientific, Waltham, MA, USA) in the 4000–500 cm^{-1} range, using a resolution of 8 cm^{-1} and 32 scans per sample.

Morphological analysis of BC by Field Emission-Scanning Electron Microscopy (FE-SEM)

The surface morphology of BC membranes was examined via FE-SEM (SIGMA, Carl Zeiss, Germany) operated at an accelerating voltage of 5 kV. The instrument provided a resolution of 1.0 nm with an emission voltage of 1.5 kV. Samples were sputter-coated with platinum to minimize charging and improve conductivity. High-resolution images were acquired at 100,000× magnification to assess the nanofibrillar architecture of BC.

Phage propagation and lysate preparation

Salmonella enterica serovar Typhimurium ST1, a pig-derived host strain (KVCC-BA2000161), was cultured overnight in tryptic soy broth (TSB; BD, Sparks, MD, USA) at 37°C with shaking at 160 rpm [41]. To amplify SLAM_phiST1N3, lytic phage in the *Cornellvirus* genus for biocontrol of a multidrug-resistant *S.* Typhimurium in the swine industry chain, 1 mL of the overnight bacterial culture was mixed with 20 mL of fresh TSB and 20 mL of phage-containing supernatant [42]. The mixture was incubated for more than 16 h at 37 °C with shaking at 160 rpm to allow phage propagation. After incubation, cultures were centrifuged at 8,000 rpm for 15 min to remove bacterial cells. The resulting supernatant was collected, passed through a 0.22 μm pore-size syringe filter (Whatman, Maidstone, England), and used as the crude phage lysate. Phage purification was performed through repeated plaque isolation and elution, followed by final sterilization by filtration. The purified lysate was used as working phage stock for all subsequent experiments.

Phage adsorption onto BC membranes

The phage lysate was buffer-exchanged into PBS (pH 7.4) and diluted to 1×10^8 PFU/mL for subsequent immobilization assays. SLAM_phiST1N3 was immobilized onto BC pellicles by physical adsorption [43]. Purified BC membranes were submerged in the phage suspension and incubated at room temperature on a tilting shaker (LaboShaker R100, Gyrozen, South Korea) at 10 rpm for 1 h. After incubation at room

temperature, membranes were rinsed with ultrapure distilled water (10977-023, Invitrogen, USA) to remove non-adsorbed phages. BC-bound phages were used immediately in antimicrobial assays [10].

Antimicrobial activity on solid media

S. Typhimurium ST1 was cultured in tryptic soy broth (TSB; BD, Sparks, MD, USA) at 37 °C with shaking at 160 rpm to prepare an indicator suspension (~10^8 CFU/mL) [42]. For the overlay, soft agar (0.75% w/v) was prepared by mixing the bacterial suspension with tryptic soy agar (TSA; 1.5% w/v agar) and overlaying onto solidified TSA plates to form a uniform bacterial lawn. The BC films (approximately 10 × 10 mm) with or without adsorbed phages were aseptically placed onto the agar surface using the spot diffusion method. After incubation at 37°C for 24 h, antimicrobial activity was evaluated by measuring zones of inhibition around BC samples.

Liquid inhibition assay

For liquid-phase inhibition, an ST1 culture was grown to $OD_{600} \approx 0.30$ (mid-log; approximately 10^8 CFU/mL), then diluted to approximately 10^6 CFU/mL in fresh TSB. A 96-well plate assay was set up with 180 µL TSB, 10 µL bacterial suspension, and 10 mg of either phage-loaded or control BC per well (final volume 200 µL). Plates were incubated at 37 °C with orbital shaking, and bacterial growth was monitored every hour for 14 h by measuring OD600 using a microplate reader. All experiments were conducted in triplicate.

Statistical analysis

Statistical analysis for the OVAT experiments was conducted using unpaired two-tailed t-tests, and p-values < 0.05 (*), < 0.01 (**), < 0.001 (***), and < 0.0001 (****) were considered statistically significant. All values are presented as the mean ± standard deviation (SD) and were obtained from three or more independent experiments. Statistical analyses, including regression modeling, analysis of variance (ANOVA), and model adequacy evaluations (R^2, adjusted R^2, and p-values), were conducted using Minitab

statistical software (Minitab, LLC, State College, PA, USA). Optimization of the significant variables was conducted using Microsoft Excel Solver to support predictive modeling and model validation.

Results

Isolation and identification of BC producing strains from Kombucha

Three bacterial strains including *K. intermedius* SLAM-NK6B, *K. rhaeticus* SLAM-JS1B, and *K. rhaeticus* SLAM-JS2B, were successfully isolated from kombucha pellicles and assessed for BC production under static aerobic conditions at 25 °C in GYM medium (Fig. 1A). The *K. rhaeticus* strains consistently exhibited more pronounced pellicle formation compared to *K. intermedius*. Whole-genome analysis of *K. intermedius* SLAM-NK6B revealed a canonical BC biosynthetic gene cluster (*bcsA–bcsB–bcsC*) at positions 3,165,943–3,174,574, along with an additional, frameshifted copy of *bcsC* located between positions 1,737,762 – 1,746,004 (Fig. 1B). Interestingly, genomic characterization of *K. rhaeticus* SLAM-JS1B indicated a *bcs* locus comprising *bcsB* and *bcsC*, with a putative glycosyltransferase family 2 (GT2) gene (Fig. 1C). Quantification of freeze-dried pellicles revealed that *K. intermedius* SLAM-NK6B produced 36.3 ± 5.3 mg/L of BC, while *K. rhaeticus* SLAM-JS1B and SLAM-JS2B yielded 120.8 ± 28.3 mg/L and 113.3 ± 15.0 mg/L, respectively (Fig. 1D). Among them, *K. rhaeticus* SLAM-JS1B demonstrated the highest productivity and was therefore selected as the representative BC producing strain for subsequent optimization experiments.

Optimization of BC production using three-step sequential and statistical approaches

1) OVAT screening

To determine the most suitable basal medium for subsequent optimization, five standard formulations were evaluated under static conditions. Among them, SM supported the highest BC production (2.045 g/L), yielding approximately 9% more than the second-best medium, MYM (1.870 g/L). BC yields from MHSM (1.388 g/L), HSM (1.158 g/L), and GYM (0.722 g/L) decreased in the following order: MHSM > HSM > GYM (Fig. 2A). The BC yield with SM was significantly higher than those with HSM and GYM ($p = 0.041$ and 0.003, respectively). A similar trend was observed for both BC yield and productivity. SM also showed the highest productivity (26%), further supporting its selection as the basal medium. Next, to assess the

influence of different carbon sources on BC production, the original carbon source in SM (glucose) was replaced with various alternatives at a concentration of 1.5%, following the OVAT approach. While all tested carbon sources supported BC production, glucose yielded the highest BC concentration (1.988 g/L), as shown in Fig. 2B. The remaining carbon sources ranked as follows: mannitol (1.925 g/L) > sucrose (1.647 g/L) > glycerol (1.539 g/L) > sorbitol (1.109 g/L) > lactose (0.694 g/L). In addition, various organic and inorganic nitrogen sources were evaluated at 1.3% (w/v) to assess their effects on BC production (Figure 2C). Among these, yeast extract supported the highest BC production (1.820 g/L), followed by peptone (1.640 g/L), tryptone (1.475 g/L), ammonium chloride (0.474 g/L), and ammonium nitrate (0.162 g/L). Notably, ammonium sulfate did not support BC production. Finally, incubation temperature was varied to identify the optimal thermal condition for BC synthesis. The highest yield was achieved at 25°C (1.926 g/L), followed by 20°C (1.758 g/L) and 30°C (1.039 g/L) (Fig. 2D). No detectable BC was produced at 15°C or 35°C, underscoring the temperature sensitivity of the strain.

2) PBD for variable screening

Based on the results of the OVAT experiments, a PBD was employed to evaluate the influence of six independent nutritional and physical variables on BC production through 12 experimental runs. Each variable was evaluated at two levels, coded as high (+1) and low (−1), and BC yield (g/L) served as the response (Table 1). The main effects analysis revealed that glucose, magnesium sulfate, ethanol, and incubation time exerted positive effects on BC production, whereas yeast extract and potassium phosphate (KH_2PO_4) had negative effects (Fig. 3A). Among the tested variables, ethanol, magnesium sulfate, and yeast extract were identified as the most significant factors influencing BC production, as confirmed by the Pareto chart (Fig. 3B). These three variables were statistically significant within the model. As the PBD relies on a first-order linear model, regression analysis yielded the following predictive equation:

$$\text{Eq. 1: Result} = 0.659 + 0.01264(X_1) - 0.02233(X_2) - 0.0257(X_3) + 0.2960(X_4) + 0.14329(X_5) + 0.00644(X_6)$$

The model exhibited a high degree of fit, with an R^2 value of 0.968 and an adjusted R^2 (adj-R^2) of 0.962, indicating strong predictive accuracy and reliability of the applied model.

3) BBD for optimized conditions

The most significant variables identified from the PBD, namely yeast extract (X_1), $MgSO_4$ (X_2), and ethanol (X_3), were further investigated using a three-level BBD to determine the optimal concentrations for maximizing BC production (Table 2). According to the regression analysis, increasing concentrations of $MgSO_4$ and ethanol had a positive effect on BC yield, whereas higher levels of yeast extract negatively influenced BC production. The interaction effects between variables on BC yield were visualized using three-dimensional surface plots (Fig. 4A, 4B, and 4C). In these plots, two independent variables were represented on the X- and Y-axes, while BC yield was plotted on the Z-axis. The third variable was held constant at its midpoint value. The regression equation derived from the BBD for predicting BC production as a second-order polynomial model is as follows:

Eq. 2: $\text{Result} = 0.570 - 0.0254(X_1) - 0.1535(X_2) + 0.0751(X_3) + 0.001093(X_1)^2 + 0.0871(X_2)^2 + 0.003053(X_3)^2 - 0.00388\,(X_1X_2) - 0.003070(X_1X_3) + 0.02466(X_2X_3)$

The BBD model demonstrated a high level of fit, with an R^2 value of 0.968 and an adjusted R^2 of 0.960, indicating good reliability and predictive capability. Using Excel's Solver function to predict the optimal conditions for maximal BC production, the best combination was determined to be 10 g/L of yeast extract, 2 g/L of $MgSO_4$, and 10 mL/L of ethanol, resulting in a predicted BC yield of 2.584 g/L. This optimized yield was 1.26 times higher than that obtained using the original Saleh medium formulation. Experimental validation of the optimized model yielded an actual BC production of 2.795 g/L, demonstrating a prediction accuracy of 92%. Overall, the final optimized medium formulation resulted in approximately a 37% improvement in BC productivity compared to the baseline SM. This result suggests the effectiveness of the multi-step optimization strategy in enhancing BC yield and process efficiency.

Physicochemical and morphological characterization of BC from *K. rhaeticus* SLAM-JS1B

The FT-IR spectrum of freeze-dried BC was compared with that of microcrystalline cellulose (MCC) as a reference (Fig. 5A). Both BC and MCC exhibited characteristic absorption bands at 3340 cm^{-1} (O–H stretching), 2900 cm^{-1} (C–H stretching), 1430 cm^{-1} (CH_2 bending), and 1060 cm^{-1} (C–O–C stretching) [44, 45]. The similarity of the spectral patterns confirms the polysaccharide nature of the produced BC and its structural consistency with native cellulose. The physiological and morphological features of BC were further analyzed by FE-SEM (Fig. 5B). The micrographs revealed a dense and interconnected nanofibrillar network with a highly porous architecture. The fibers were randomly oriented and extensively entangled, forming a mesh-like structure typical of microbial cellulose. This nanoarchitecture offers a large surface area and open porosity, providing favorable conditions for functionalization and biomolecule immobilization.

Phage immobilized BC and antimicrobial activity against *S.* Typhimurium

Given the porous and highly entangled nanofibrillar structure, the BC matrix was investigated as a potential carrier for phage delivery. SEM imaging of phage-loaded BC confirmed the successful adsorption of *S.* Typhimurium ST1 phages onto cellulose fibrils, with distinct phage particles clearly visualized on the nanofiber surfaces (Fig. 6A and 6B). The phages were found to be immobilized and entrapped within the BC at a level of 5.8 ± 0.3 log particles/mm^2 (Fig. 6C). The antimicrobial efficacy of phage immobilized BC (phage–BC) phagewas evaluated using a lawn inhibition assay. While native BC exerted no detectable inhibitory effect against *S.* Typhimurium (Fig. 6D), BC samples immobilized with SLAM_phiST1N3 lytic phage produced clear inhibition zones, confirming the retained infectivity and lytic capacity of the entrapped phages (Fig. 6E). In broth, phage–BC markedly suppressed the growth of *S.* Typhimurium ST1 during the early phase of incubation relative to the control (Fig. 6F). Specifically, OD_{600} remained near baseline for approximately 2 h and increased only modestly thereafter, reaching 0.248 ± 0.014 at 4 h, compared to 0.620 ± 0.006 in the untreated control ($p<0.05$). The time to reach $OD_{600} = 0.5$ was delayed by

approximately 3 h in the phage-treated group, indicating a pronounced early antibacterial effect. Between 6 and 10 h, bacterial growth resumed, and OD_{600} values approached those of the control group by 10–12 h, reflecting partial regrowth after phage-induced lysis. Integrated growth ($AUC_{0\text{-}6h}$) was reduced by 56.8% in the BC-treated group compared with the control (2.805 vs. 1.211 OD·h; trapezoidal rule on hourly OD_{600} means).

Discussion

In this study, we established a stepwise, statistically grounded optimization strategy combining OVAT, PBD, and BBD to enhance BC production by *K. rhaeticus* SLAM-JS1B. Using Saleh medium as the baseline reference, initial screening identified glucose and yeast extract as effective carbon and nitrogen sources, respectively, and indicated 25 °C as the optimal cultivation temperature under static conditions. Building on these insights, PBD highlighted ethanol, $MgSO_4$, and yeast extract as the principal variables affecting BC yield, and subsequent BBD quantified their individual and interactive effects. The final optimized formulation consisted of 10 g/L yeast extract, 2 g/L $MgSO_4$, and 10 mL/L ethanol, with glucose and KH_2PO_4 maintained at their design-space levels. This recipe yielded an experimentally validated BC yield of 2.795 g/L, representing approximately a 37% improvement over the baseline. Notably, the optimized formulation reduced nitrogen input while enhancing productivity, offering both economic and environmental advantages. Although *K. intermedius* SLAM-NK6B also produced BC, *K. rhaeticus* SLAM-JS1B demonstrated superior yield and consistency under identical conditions.

We therefore designated *K. rhaeticus* SLAM-JS1B as the primary experimental strain and implemented a stepwise optimization strategy to enhance BC production. A notable outcome of the screening and modeling sequence was the asymmetric role of nitrogen: moderate levels of yeast extract supported robust production, whereas concentrations exceeding the optimum were associated with reduced yields. This pattern is consistent with a metabolic shift toward biomass accumulation rather than BC synthesis when nitrogen is in excess [46]. By contrast, ethanol and $MgSO_4$ exerted positive, dose-dependent effects on BC production. The stimulatory response to ethanol is consistent with prior observations that ethanol can modulate carbon flux toward UDP-glucose–dependent routes and suppress competing pathways [47, 48]. Meanwhile, Mg^{2+} is known to support carbohydrate-metabolizing enzymes and the activity of cellulose synthase regulated by c-di-GMP [49]. Reports on related *Acetobacter* and *Komagataeibacter* strains that associate Mg^{2+} availability with increased BC yield further support this interpretation [50, 51]. Although these mechanistic links align with previous reports, transcriptomic or metabolomic analyses would be

required to confirm these pathways in *K. rhaeticus* SLAM-JS1B. The BBD-derived model captured both curvature and interaction terms, enabling interpolation within the experimental domain and yielding predictions that closely matched the validation experiments (prediction accuracy approximately 92%). This approach enables informed fine-tuning of medium composition without reliance on trial and error. Since all experiments were conducted under static flask conditions, translating these findings to bioreactor systems will require adaptation to controlled pH and oxygenation, as well as evaluations of batch reproducibility and scale-up robustness. The trends observed during preliminary screening were consistent with general metabolic expectations and previous reports. Glucose outperformed other carbon sources, likely reflecting its efficient entry into glycolysis and enhanced precursor availability for cellulose biosynthesis [52, 53]. Interestingly, mannitol's performance is compatible with slower catabolism and reduced byproduct formation [54], whereas lactose yielded the lowest BC titers, likely reflecting limited capacity to hydrolyze β-1,4-glycosidic bonds without specific hydrolases [55, 56]. Among nitrogen sources, complex nitrogen sources (yeast extract, peptone, tryptone) supported higher production, consistent with their provision of amino acids, vitamins, and cofactors that benefit growth and cellulose synthesis [57], whereas inorganic sources performed poorly and ammonium sulfate failed to support detectable synthesis, in line with earlier observations [52, 58, 59]. Other variables, such as glucose concentration, KH_2PO_4, and incubation time, showed relatively minor effects within the tested ranges. Temperature profiling further confirmed 25 °C as optimal, with BC production ceasing at 15 °C and 35 °C, consistent with the mesophilic nature of *Komagataeibacter* and the temperature sensitivity of cellulose biosynthetic pathways [60, 61].

Structural and physicochemical characterization of the BC confirmed that the cellulose produced under the optimized conditions exhibits the chemical signatures and nanoscale morphology typical of high-purity BC. The FT-IR spectra exhibited cellulose-specific absorption bands near 3340, 2900, 1430, and 1060 cm^{-1} [62], and the absence of lignin- or hemicellulose-associated peaks indicated high purity [63]. FE-SEM analysis revealed a dense, randomly oriented nanofibrillar network with fiber diameters ranging from 50 to 200 nm, consistent with reported morphologies of high-quality *Komagataeibacter*-derived BC. [64]. To evaluate its functional properties, we immobilized lytic phages targeting *S.* Typhimurium onto the BC

matrix [65-67]. *S.* Typhimurium is a major enteric pathogen affecting a wide range of livestock species, including ruminants such as cattle, sheep, and goats, and it has been frequently isolated from their intestinal tracts [68, 69]. In particular, infection in young or immunocompromised animals can result in acute enteritis, dehydration, and growth retardation, underscoring the pathogen's significant impact on animal health and productivity [70, 71]. Therefore, beyond its role as a dietary fiber comparable to conventional roughage, phage–BC offers preventive potential against enteric diseases in livestock.

Electron micrographs confirmed the successful attachment of *S.* Typhimurium phages to the BC nanofibrillar network, while antimicrobial assays showed that phages immobilized within BC retained infectivity against the pathogen. These findings indicate that BC can serve as a biocompatible, structurally stable delivery matrix for bioactive agents [72]. The antimicrobial efficacy of phage–BC against *S.* Typhimurium suggests potential to reduce pathogen load in livestock, thereby improving gut health, feed efficiency, and overall production performance while reducing reliance on conventional antibiotics [14]. Given its physicochemical properties and compatibility with phage immobilization, BC may be a promising carrier for antimicrobial delivery in livestock applications, particularly for targeted interventions in animal production systems [73-76].

Taken together, the sequential and statistically grounded strategy (OVAT, followed by PBD and BBD) enabled the rational identification of key medium components, defined their optimal levels, and significantly enhanced BC yields without compromising material quality. This integrative approach provides a robust framework for strain-specific optimization of culture conditions and establishes a foundation for downstream studies on large-scale production, cost modeling, and the functional deployment of BC in antimicrobial applications within the animal industry.

Acknowledgment

This project was supported in part by grants from a National Research Foundation of Korea Grant, funded by the Korean government (MEST; 2021R1A2C3011051) and by the support of "Cooperative Research

Program for Agriculture Science and Technology Development (Project No. RS-2025-02263976)" Rural Development Administration, Republic of Korea.

References

1. Abdelraof M, Hasanin MS, Farag MM, Ahmed HY. Green synthesis of bacterial cellulose/bioactive glass nanocomposites: Effect of glass nanoparticles on cellulose yield, biocompatibility and antimicrobial activity. Int J Biol Macromol. 2019;138:975-85.
2. McNamara JT, Morgan JL, Zimmer J. A molecular description of cellulose biosynthesis. Annual review of biochemistry. 2015;84(1):895-921.
3. Chopra L. Extraction of cellulosic fibers from the natural resources: A short review. Materials Today: Proceedings. 2022;48:1265-70.
4. Mohammadkazemi F, Azin M, Ashori A. Production of bacterial cellulose using different carbon sources and culture media. Carbohyd Polym. 2015;117:518-23.
5. Lee S-B, Nejad JG, Lee HG. Supplemental effects of rumen-protected L-tryptophan at various levels on starch digestion, melatonin and gastrointestinal hormones in Holstein steers. Journal of Animal Science and Technology. 2025;67(1):86.
6. Sun M, Han H, Zhang X, Liu H, Ding H, Liu X, et al. Reducing methane emissions in Tibetan sheep at high altitudes through indoor feeding of a low-fibre total mixed pellet diet. Journal of Animal Science and Technology. 2025.
7. Kim M, Park T, Park C, Baek Y-C, Cho A, Lee HG, et al. Impact of rumen cannulation surgery on rumen microbiota composition in Hanwoo steers. Journal of animal science and technology. 2024;66(2):353.
8. Kang R, Lee H, Seon H, Park C, Song J, Park JK, et al. Effects of diets for three growing stages by rumen inocula donors on in vitro rumen fermentation and microbiome. Journal of Animal Science and Technology. 2024;66(3):523.
9. Girard VD, Chaussé J, Vermette P. Bacterial cellulose: A comprehensive review. Journal of applied polymer science. 2024;141(15):e55163.
10. Huang Y-C, Khumsupan D, Lin S-P, Santoso SP, Hsu H-Y, Cheng K-C. Production of bacterial cellulose (BC)/nisin composite with enhanced antibacterial and mechanical properties through co-cultivation of Komagataeibacter xylinum and Lactococcus lactis subsp. lactis. International Journal of Biological Macromolecules. 2024;258:128977.
11. Naomi R, Bt Hj Idrus R, Fauzi MB. Plant-vs. Bacterial-derived cellulose for wound healing: A review. International journal of environmental research and public health. 2020;17(18):6803.
12. Kim ES, Cho JH, Song M, Kim S, Keum GB, Doo H, et al. Genome analysis of Lactococcus taiwanensis strain K_LL001 with potential cellulose degrading functions. Journal of Animal Science and Technology. 2025;67(1):273.
13. Yoon S, Moon J, Kim H, Seo J. Development and characterization of endolysin SALys78925 with antimicrobial activity against Streptococcus agalactiae. Journal of Animal Science and Technology. 2025.
14. Choi Y, Kang A, Kang M-G, Lee DJ, Kyoung D, Kwak M-J, et al. Exploring synergistic effect of bacteriophages with probiotics against multidrug resistant Salmonella Typhimurium in a simulated chicken gastrointestinal system using metagenomic- and culturomic approaches. Journal of Animal Science and Technology. 2025.
15. Song D, Lee J, Kim K, Oh H, An J, Chang S, et al. Erratum to: Effects of dietary supplementation of Pediococcus pentosaceus strains from kimchi in weaned piglet challenged with Escherichia coli and Salmonella enterica. Journal of Animal Science and Technology. 2025;67(2):494.
16. Mellor KC, Petrovska L, Thomson NR, Harris K, Reid SW, Mather AE. Antimicrobial resistance diversity suggestive of distinct Salmonella Typhimurium sources or selective pressures in food-production animals. Frontiers in Microbiology. 2019;10:708.
17. Rackov N, Janßen N, Akkache A, Drotleff B, Beyer B, Scoppola E, et al. Bacterial cellulose: Enhancing productivity and material properties through repeated harvest. Biofilm. 2025;9:100276.

18. Cruz MA, Flor-Unda O, Avila A, Garcia MD, Cerda-Mejía L. Advances in bacterial cellulose production: a scoping review. Coatings. 2024;14(11):1401.
19. Zhong C. Industrial-scale production and applications of bacterial cellulose. Frontiers in Bioengineering and Biotechnology. 2020;8:605374.
20. Florea M, Hagemann H, Santosa G, Abbott J, Micklem CN, Spencer-Milnes X, et al. Engineering control of bacterial cellulose production using a genetic toolkit and a new cellulose-producing strain. Proceedings of the National Academy of Sciences. 2016;113(24):E3431-E40.
21. Vigentini I, Fabrizio V, Dellacà F, Rossi S, Azario I, Mondin C, et al. Set-up of bacterial cellulose production from the genus Komagataeibacter and its use in a gluten-free bakery product as a case study. Frontiers in microbiology. 2019;10:1953.
22. Hestrin S, Schramm M. Synthesis of cellulose by Acetobacter xylinum. 2. Preparation of freeze-dried cells capable of polymerizing glucose to cellulose. Biochemical Journal. 1954;58(2):345.
23. Tseng YS, Patel AK, Chen C-W, Dong C-D, Singhania RR. Improved production of bacterial cellulose by Komagataeibacter europaeus employing fruit extract as carbon source. Journal of Food Science and Technology. 2023;60(3):1054-64.
24. Cardoso VM, Campani G, Santos MP, Silva GG, Pires MC, Gonçalves VM, et al. Cost analysis based on bioreactor cultivation conditions: Production of a soluble recombinant protein using Escherichia coli BL21 (DE3). Biotechnology Reports. 2020;26:e00441.
25. Bagewadi ZK, Bhavikatti JS, Muddapur UM, Yaraguppi DA, Mulla SI. Statistical optimization and characterization of bacterial cellulose produced by isolated thermophilic Bacillus licheniformis strain ZBT2. Carbohyd Res. 2020;491.
26. Saleh AK, Soliman NA, Farrag AA, Ibrahim MM, El-Shinnawy NA, Abdel-Fattah YR. Statistical optimization and characterization of a biocellulose produced by local Egyptian isolate AS.5. Int J Biol Macromol. 2020;144:198-207.
27. Yatsyshyn VY, Fedorovych DV, Sibirny AA. Medium optimization for production of flavin mononucleotide by the recombinant strain of the yeast using statistical designs. Biochem Eng J. 2010;49(1):52-60.
28. Plackett RL, Burman JP. The design of optimum multifactorial experiments. Biometrika. 1946;33:305-25.
29. Bae S, Shoda M. Statistical optimization of culture conditions for bacterial cellulose production using Box-Behnken design. Biotechnol Bioeng. 2005;90(1):20-8.
30. Choi Y, Lee W, Kwon J-G, Kang A, Kwak M-J, Eor J-Y, et al. The current state of phage therapy in livestock and companion animals. Journal of Animal Science and Technology. 2024;66(1):57.
31. Kang M-G, Kwak M-J, Kang A, Park J, Lee DJ, Mun J, et al. Metagenome-based microbial metabolic strategies to mitigate ruminal methane emissions using Komagataeibacter-based symbiotics. Science of The Total Environment. 2025;987:179793.
32. Kang M-G, Kwak M-J, Kim Y. Polystyrene Microplastics Biodegradation by Gut Bacterial Enterobacter hormaechei From Mealworms Under Anaerobic Conditions: Anaerobic Oxidation and Depolymerization. Journal of Hazardous Materials. 2023:132045.
33. Kim K, Lee J, Oh S. Whole Genome Sequence Analysis of Bifidobacterium animalis subsp. lactis KL101 and Comparative Genomics with BB12. Journal of Animal Science and Technology. 2024.
34. Baik KS, Ramos SC, Na SH, Kim SH, Son AR, Miguel M, et al. Complete genome sequence of Corynebacterium sp. SCR221107, encoding biosynthesis of vitamin B12 isolated from the rumen fluid of Holstein dairy cows. Journal of Animal Science and Technology. 2024;66(6):1291.
35. Ryu S, Doo H, Kim ES, Keum GB, Kwak J, Pandey S, et al. Complete genome sequence of Lactiplantibacillus plantarum strain GA_C_14 with potential characteristics applicable in the swine industry. Journal of Animal Science and Technology. 2025;67(4):944.
36. Lee I, Ouk Kim Y, Park S-C, Chun J. OrthoANI: an improved algorithm and software for calculating average nucleotide identity. International journal of systematic and evolutionary microbiology. 2016;66(2):1100-3.

37. Feng X, Ge Z, Wang Y, Xia X, Zhao B, Dong M. Production and characterization of bacterial cellulose from kombucha-fermented soy whey. Food Production, Processing and Nutrition. 2024;6(1):20.
38. Schramm M, Hestrin S. Synthesis of Cellulose by Acetobacter-Xylinum .1. Micromethod for the Determination of Celluloses. Biochemical Journal. 1954;56(1):163-6.
39. Yamanaka S, Watanabe K, Kitamura N, Iguchi M, Mitsuhashi S, Nishi Y, et al. The Structure and Mechanical-Properties of Sheets Prepared from Bacterial Cellulose. J Mater Sci. 1989;24(9):3141-5.
40. Saleh AK, El-Gendi H, Soliman NA, El-Zawawy WK, Abdel-Fattah YR. Bioprocess development for bacterial cellulose biosynthesis by novel
isolate along with characterization and antimicrobial assessment of fabricated membrane. Sci Rep-Uk. 2022;12(1).
41. Song D, Lee J, Kim K, Oh H, An J, Chang S, et al. Effects of dietary supplementation of Pediococcus pentosaceus strains from kimchi in weaned piglet challenged with Escherichia coli and Salmonella enterica. Journal of Animal Science and Technology. 2023;65(3):611.
42. Choi Y, Kwak M-J, Kang M-G, Kang AN, Lee W, Mun D, et al. Molecular characterization and environmental impact of newly isolated lytic phage SLAM_phiST1N3 in the Cornellvirus genus for biocontrol of a multidrug-resistant Salmonella Typhimurium in the swine industry chain. Science of The Total Environment. 2024;922:171208.
43. Farooq U, Ullah MW, Yang Q, Aziz A, Xu J, Zhou L, et al. High-density phage particles immobilization in surface-modified bacterial cellulose for ultra-sensitive and selective electrochemical detection of Staphylococcus aureus. Biosensors and Bioelectronics. 2020;157:112163.
44. Rusdi RAA, Halim NA, Nurazzi MN, Abidin ZHZ, Abdullah N, Che Ros F, et al. Pre-treatment effect on the structure of bacterial cellulose from Nata de Coco (Acetobacter xylinum). Polimery. 2022;67(3):110-8.
45. Umamaheswari S, Malkar O, Naveena K. FTIR spectral and microarchitectural analysis of cellulose produced by Lactococcus lactis under agitated condition. Journal of Pure and Applied Microbiology. 2017;11(4):1965-72.
46. Zhang H, Chen C, Zhu C, Sun D. Production of bacterial cellulose by Acetobacter xylinum: Effects of carbon/nitrogen-ratio on cell growth and metabolite production. Cellulose Chem Technol. 2016;50(9):997-1003.
47. Ryngajllo M, Jacek P, Cielecka I, Kalinowska H, Bielecki S. Effect of ethanol supplementation on the transcriptional landscape of bionanocellulose producer Komagataeibacter xylinus E25. Appl Microbiol Biot. 2019;103(16):6673-88.
48. Montenegro-Silva P, Ellis T, Dourado F, Gama M, Domingues L. Enhanced bacterial cellulose production in
: impact of different PQQ-dependent dehydrogenase knockouts and ethanol supplementation. Biotechnol Biof Biop. 2024;17(1).
49. Mohite BV, Salunke BK, Patil SV. Enhanced Production of Bacterial Cellulose by Using
NCIM 2529 Strain Under Shaking Conditions. Applied Biochemistry and Biotechnology. 2013;169(5):1497-511.
50. Fontana JD, Joerke CG, Baron M, Maraschin M, Ferreira AG, Torriani I, et al. Acetobacter cellulosic biofilms search for new modulators of cellulogenesis and native membrane treatments. Applied biochemistry and biotechnology. 1997;63:327-38.
51. Heo MS, Son HJ. Development of an optimized, simple chemically defined medium for bacterial cellulose production by
sp A9 in shaking cultures. Biotechnol Appl Bioc. 2002;36:41-5.
52. Thongwai N, Futui W, Ladpala N, Sirichai B, Weechan A, Kanklai J, et al. Characterization of Bacterial Cellulose Produced by
P285 Isolated from Contaminated Honey Wine. Microorganisms. 2022;10(3).
53. Son HJ, Heo MS, Kim YG, Lee SJ. Optimization of fermentation conditions for the production of bacterial cellulose by a newly isolated
sp A9 in shaking cultures. Biotechnol Appl Bioc. 2001;33:1-5.

54. Płoska J, Garbowska M, Klempová S, Stasiak-Różańska L. Obtaining Bacterial Cellulose through Selected Strains of Acetic Acid Bacteria in Classical and Waste Media. Applied Sciences. 2023;13(11):6429.
55. Nguyen VT, Flanagan B, Gidley MJ, Dykes GA. Characterization of Cellulose Production by a Strain from Kombucha. Curr Microbiol. 2008;57(5):449-53.
56. Jozala AF, Pértile RAN, dos Santos CA, Santos-Ebinuma VD, Seckler MM, Gama FM, et al. Bacterial cellulose production by by employing alternative culture media. Appl Microbiol Biot. 2015;99(3):1181-90.
57. Son H-J, Kim H-G, Kim K-K, Kim H-S, Kim Y-G, Lee S-J. Increased production of bacterial cellulose by Acetobacter sp. V6 in synthetic media under shaking culture conditions. Bioresource technology. 2003;86(3):215-9.
58. Cielecka I, Ryngajllo M, Maniukiewicz W, Bielecki S. Highly Stretchable Bacterial Cellulose Produced by SI1. Polymers-Basel. 2021;13(24).
59. Chai J, Adnan A, editors. Effect of different nitrogen source combinations on microbial cellulose production by Pseudomonas aeruginosa in batch fermentation. IOP Conference Series: Materials Science and Engineering; 2018: IOP Publishing.
60. Ugurel C, Ögüt H. Optimization of Bacterial Cellulose Production by K23. Fibers. 2024;12(3).
61. Girard VD, Chaussé J, Vermette P. Bacterial cellulose: A comprehensive review. J Appl Polym Sci. 2024;141(15).
62. Atykyan N, Revin V, Shutova V. Raman and FT-IR Spectroscopy investigation the cellulose structural differences from bacteria Gluconacetobacter sucrofermentans during the different regimes of cultivation on a molasses media. Amb Express. 2020;10(1):84.
63. Rostamabadi H, Bist Y, Kumar Y, Yildirim‐Yalcin M, Ceyhan T, Falsafi SR. Cellulose nanofibers, nanocrystals, and bacterial nanocellulose: Fabrication, characterization, and their most recent applications. Future Postharvest and Food. 2024;1(1):5-33.
64. Fatima A, Ortiz-Albo P, Neves LA, Nascimento FX, Crespo JG. Biosynthesis and characterization of bacterial cellulose membranes presenting relevant characteristics for air/gas filtration. Journal of Membrane Science. 2023;674:121509.
65. Choi Y, Kang A, Kang M-G, Lee DJ, Kyoung D, Kwak M-J, et al. Exploring synergistic effect of bacteriophages with probiotics against multidrug resistant Salmonella Typhimurium in a simulated chicken gastrointestinal system using metagenomic-and culturomic approaches. Journal of Animal Science and Technology. 2025.
66. Song D, Lee J, Yoo Y, Oh H, Chang S, An J, et al. Effects of probiotics on growth performance, intestinal morphology, intestinal microbiota weaning pig challenged with Escherichia coli and Salmonella enterica. Journal of Animal Science and Technology. 2025;67(1):106.
67. Kim H, Lee J, Kim S, Kim B, Chang S, Song D, et al. Supplemental illite or in combination with probiotics improves performance and gut health in broilers challenged with Salmonella typhimurium. Journal of Animal Science and Technology. 2024.
68. Tadesse G, Tessema TS. A meta-analysis of the prevalence of Salmonella in food animals in Ethiopia. BMC microbiology. 2014;14(1):270.
69. Kim H, Lee J, Kim S, Kim B, Chang S, Song D, et al. Supplemental illite or in combination with probiotics improves performance and intestinal health in broiler chickens challenged with Salmonella typhimurium. Journal of Animal Science and Technology. 2025;67(5):1033.
70. Muktar Y, Mamo G, Tesfaye B, Belina D. A review on major bacterial causes of calf diarrhea and its diagnostic method. Journal of Veterinary Medicine and Animal Health. 2015;7(5):173-85.
71. Choi IY, Park DH, Chin BA, Lee C, Lee J, Park M-K. Exploring the feasibility of Salmonella Typhimurium-specific phage as a novel bio-receptor. Journal of animal science and technology. 2020;62(5):668.

72. Jo H, Han G, Kim EB, Kong C, Kim BG. Effects of supplemental bacteriophage on the gut microbiota and nutrient digestibility of ileal-cannulated pigs. Journal of animal science and technology. 2024;66(2):340.
73. Joo YH, Baeg CH, Kim JY, Choi BG, Paradhipta DHV, Kim DH, et al. Effects of dietary protected fat and vitamin E on in vitro rumen fermentation characteristics and reproductive performances of Hanwoo cows. Journal of Animal Science and Technology. 2025;67(3):581.
74. Li W, Murphy B, Larsen A. Caecum transcriptome and associated microbial community in young calves with artificial dosing of rumen content obtained from an adult cow. Journal of Animal Science and Technology. 2024.
75. Lee S, Kim J, Baek Y, Seong P, Song J, Kim M, et al. Effects of different feeding systems on ruminal fermentation, digestibility, methane emissions, and microbiota of Hanwoo steers. Journal of Animal Science and Technology. 2023;65(6):1270.
76. Zhang Y, Liang S, Choi S, Li G. Effects of maternal rumen microbiota on the development of the microbial communities in the gastrointestinal tracts of neonatal sika deer. Journal of Animal Science and Technology. 2025;67(3):619.

Table 1. Experimental levels of six variables tested by Plackett–Burman design (PBD) for optimizing BC production from *Komagataeibacter rhaeticus* SLAM-JS1B

Trails	Variables*						Response
	Glucose (X_1)	Yeast extract (X_2)	KH_2PO_4 (X_3)	$MgSO_4$ (X_4)	Ethanol (X_5)	Incubation Time (X_6)	BC (g/L)
1	1(20)	-1(10)	1(5)	-1(1)	-1(0)	-1(8)	0.725
2	1(20)	1(20)	-1(1)	1(2)	-1(0)	-1(8)	0.790
3	-1(10)	1(20)	1(5)	-1(1)	1(10)	-1(8)	1.430
4	1(20)	-1(10)	1(5)	1(2)	-1(0)	1(14)	1.005
5	1(20)	1(20)	-1(1)	1(2)	1(10)	-1(8)	2.270
6	1(20)	1(20)	1(5)	-1(1)	1(10)	1(14)	1.781
7	-1(10)	1(20)	1(5)	1(2)	-1(0)	1(14)	0.776
8	-1(10)	-1(10)	1(5)	1(2)	1(10)	-1(8)	2.149
9	-1(10)	-1(10)	-1(1)	1(2)	1(10)	1(14)	2.272
10	1(20)	-1(10)	-1(1)	-1(1)	1(10)	1(14)	1.881
11	-1(10)	1(20)	-1(1)	-1(1)	-1(0)	1(14)	0.513
12	-1(10)	-1(10)	-1(1)	-1(1)	-1(0)	-1(8)	0.666

Variables*: X_1–X_6 (variable); the coded low and high level are presented as − 1 and 1, respectively. Variable levels are presented between brackets expressed as g/L for X_1–X_4; ml for X_5; and days for X_6.

Table 2. Experimental levels of three variables tested by Box–Behnken design (BBD) for optimizing BC production from *Komagataeibacter rhaeticus* SLAM-JS1B

Trails	Variables*			Response
	Yeast extract (X_1)	$MgSO_4$ (X_2)	Ethanol (X_3)	BC (g/L)
1	-1(10)	-1(1)	0(5)	0.480
2	1(20)	-1(1)	0(5)	0.574
3	-1(10)	1(2)	0(5)	0.523
4	1(20)	1(2)	0(5)	0.605
5	-1(10)	0(1.5)	-1(0)	0.092
6	1(20)	0(1.5)	-1(0)	0.136
7	-1(10)	0(1.5)	1(10)	1.231
8	1(20)	0(1.5)	1(10)	0.968
9	0(15)	-1(1)	-1(0)	0.120
10	0(15)	1(2)	-1(0)	0.137
11	0(15)	-1(1)	1(10)	0.952
12	0(15)	1(2)	1(10)	1.196
13	0(15)	0(1.5)	0(5)	0.528
14	0(15)	0(1.5)	0(5)	0.473
15	0(15)	0(1.5)	0(5)	0.508

Variables*: X_1–X_3 (variable); the coded low and high level are presented as − 1 and 1, respectively. Variable levels are presented between brackets expressed as g/L for X_1 and X_2; ml for X_3.

Figure legends

Figure 1. Isolation of bacterial cellulose-producing strains from Kombucha. (A) Representative images of BC pellicles formed *by Komagataeibacter intermedius* SLAM-NK6B, *K. rhaeticus* SLAM-JS1B, and *K. rhaeticus* SLAM-JS2B after static aerobic cultivation at 25 °C in GYM medium. (B) Comparison of BC yields determined by the dry weight of freeze-dried pellicles. *K. rhaeticus* strains exhibited significantly higher BC production than *K. intermedius*. Among them, *K. rhaeticus* SLAM-JS1B demonstrated the highest productivity (120.8 ± 28.3 mg/L) and was selected for subsequent optimization studies. Error bars represent SD of triplicate experiments. (C) Circular whole-genome map of *K. rhaeticus* SLAM-JS1B showing co-localized *bcsB*/*bcsC* (394,990–401,545), a distal *bcsB* (769,280–770,182), and a GT2 gene (1,908,247–1,908,963). Inner track shows GC content. Whole-genome plots in (B–C) were generated with Proksee. (D) Bacterial cellulose yield (mg/L; dry weight of freeze-dried pellicles) for the three strains cultivated statically at 25°C in GYM medium. Bars indicate mean ± SD (n = 3): SLAM-NK6B, 36.3 ± 5.3; SLAM-JS1B, 120.8 ± 28.3; SLAM-JS2B, 113.3 ± 15.0.

Figure 2. Screening of medium components and cultivation conditions for BC production by *Komagataeibacter rhaeticus* SLAM-JS1B. (A) Comparison of BC yields among different basal media (SM, HSM, and GYM). SM exhibited significantly higher productivity than HSM ($p = 0.041$) and GYM ($p = 0.003$). (B) Evaluation of carbon sources for BC production. Glucose led to significantly greater yields compared to lactose ($p = 0.002$) and sorbitol ($p = 0.016$). (C) Assessment of nitrogen sources revealed that yeast extract significantly outperformed NH_4NO_3 ($p = 0.0001$) and NH_4Cl ($p = 0.0006$) in supporting BC biosynthesis. (D) Effect of incubation temperature on BC production. The optimal temperature was 25°C, which yielded significantly more BC than 20°C ($p = 0.038$) and 30°C ($p = 0.016$). Data are expressed as mean ± standard error (SEM). Statistical analysis was performed using unpaired (two-tailed) t-tests, and differences were considered significant at $p < 0.05$ (*), $p < 0.01$ (**), $p < 0.001$ (***), and $p < 0.0001$ (****)

Figure 3. Identification of significant factors affecting *Komagataeibacter rhaeticus* derived BC production using Plackett–Burman Design (PBD). (A) Main effects plot showing the direct impact of individual variables (each at coded levels of −1 and +1) on BC yield, as defined in Table 1. Positive values indicate a stimulatory effect on BC production, whereas negative values represent inhibitory effects. (B) Pareto chart illustrating the relative contribution of each variable to the overall variability in BC yield. The chart ranks culture components and conditions in descending order of influence, with a cumulative impact accounting for 100% of observed variation.

Figure 4. Interaction effects of selected medium components on *Komagataeibacter rhaeticus* derived BC biosynthesis using 3D response surface plots of yeast extract, $MgSO_4$, and ethanol. (A) Interaction between yeast extract and $MgSO_4$, (B) Interaction between yeast extract and ethanol, (C) Interaction between $MgSO_4$ and ethanol.

Figure 5. Structural, physicochemical and morphological comparison between *Komagataeibacter rhaeticus* derived BC and commercial cellulose. (A) FT-IR spectrum and (B) FE-SEM analysis of BC produced by *K. rhaeticus* and microcrystalline cellulose.

Figure 6. Phage immobilization on *Komagataeibacter rhaeticus* derived bacterial cellulose (BC) and evaluation of antimicrobial activity. (A) SEM image of native BC. (B) SEM image of phage–BC (red arrows indicate particle-like features consistent with bound phage. (C) Quantification of immobilized phage density (log particles $\times$ mm^{-2}). (D) Antimicrobial assay with native BC (no inhibition). (E) Antimicrobial assay with phage–BC (distinct lysis zones). (F) Liquid inhibition assay in TSB at 37°C with orbital shaking: growth curves (OD_{600}) of native BC (control) and phage–BC (blue). Points are mean ± SD (n = 3 technical replicates).

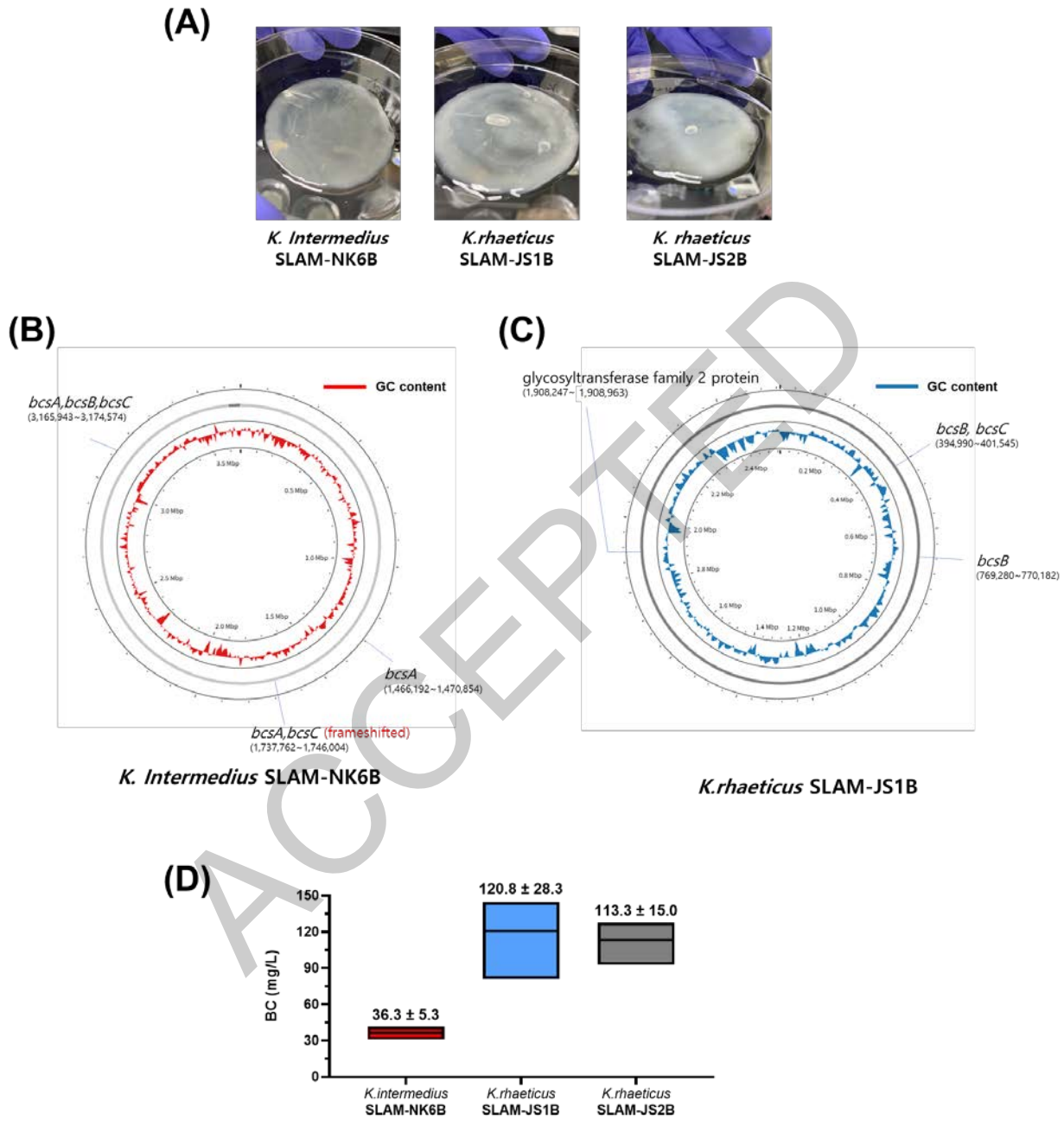

Fig. 1.

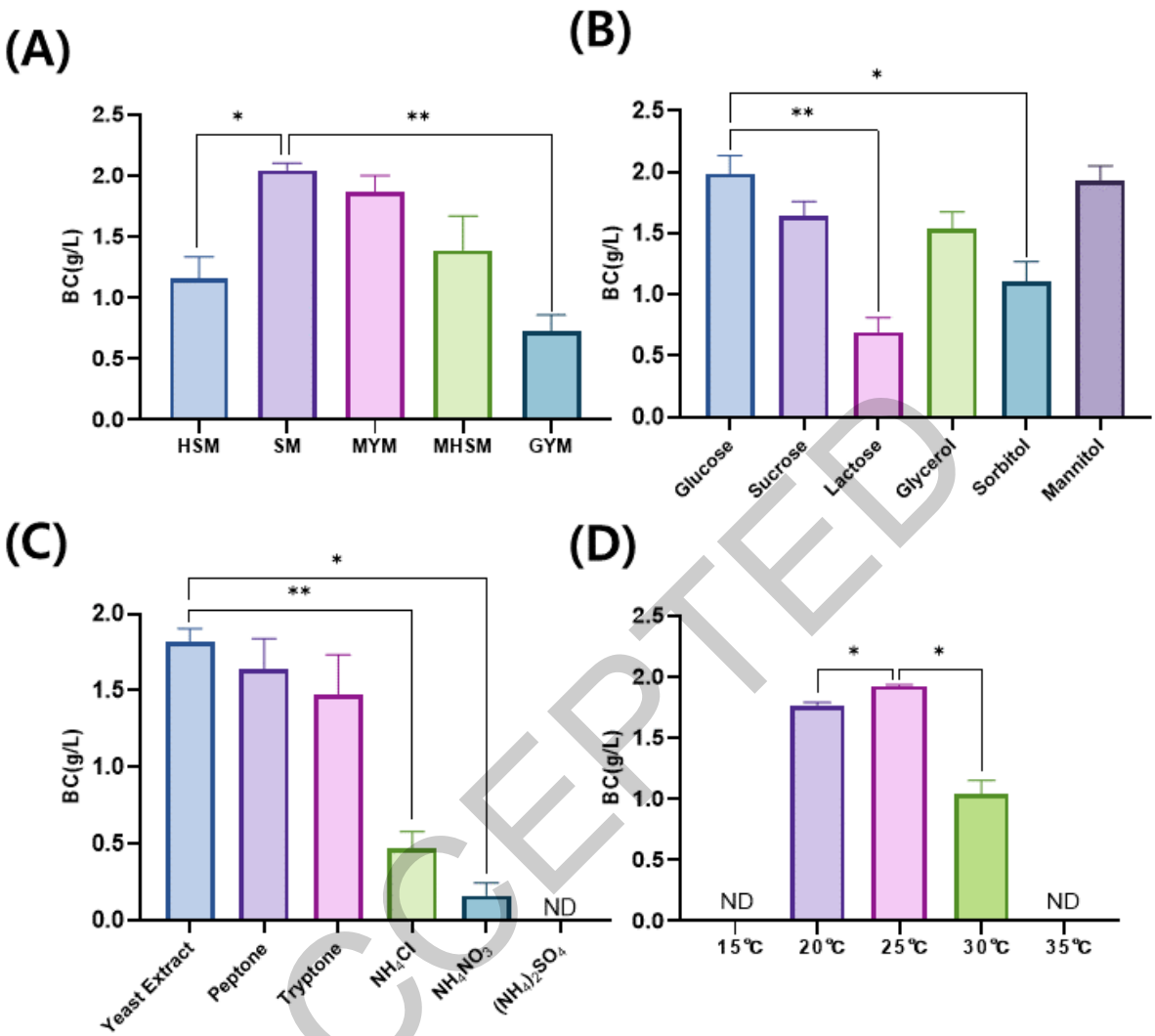

Fig. 2.

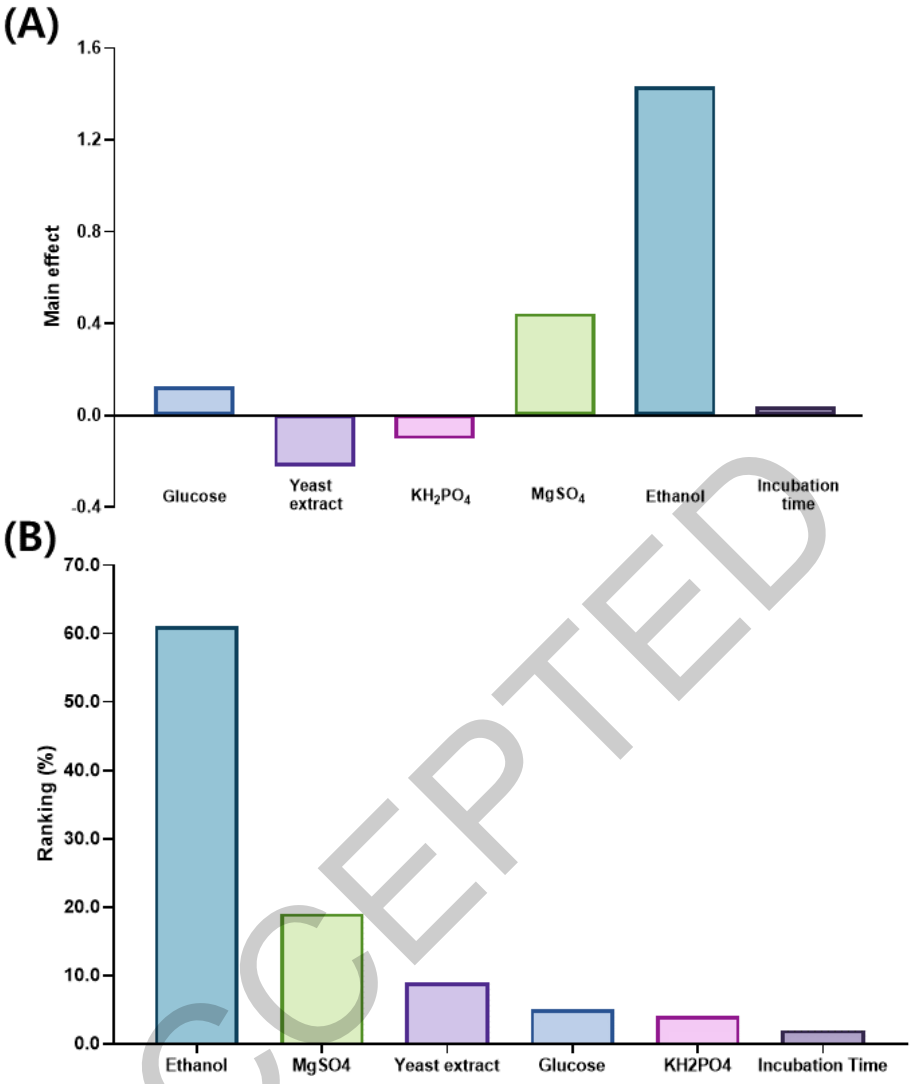

Fig. 3.

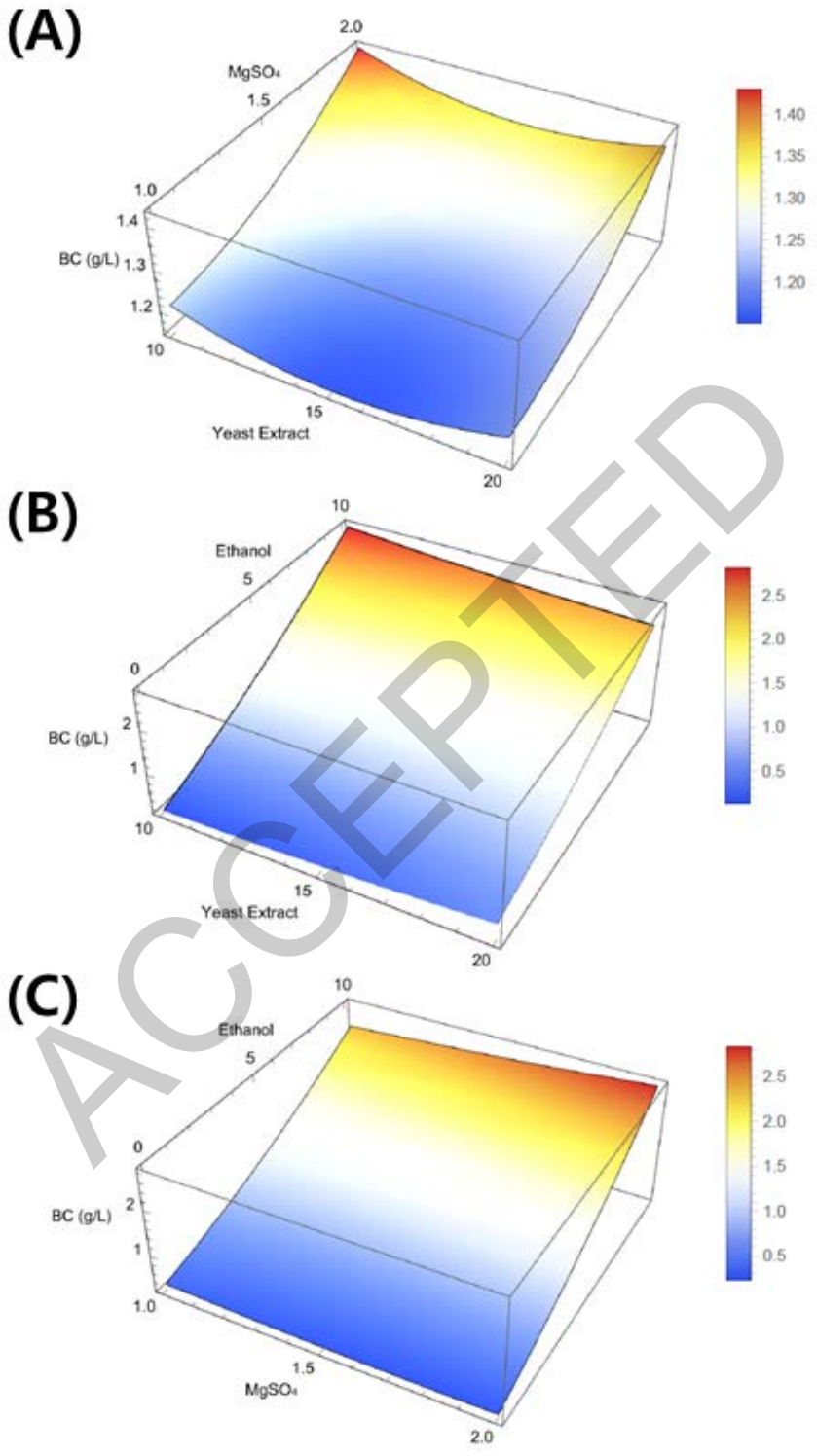

Fig. 4.

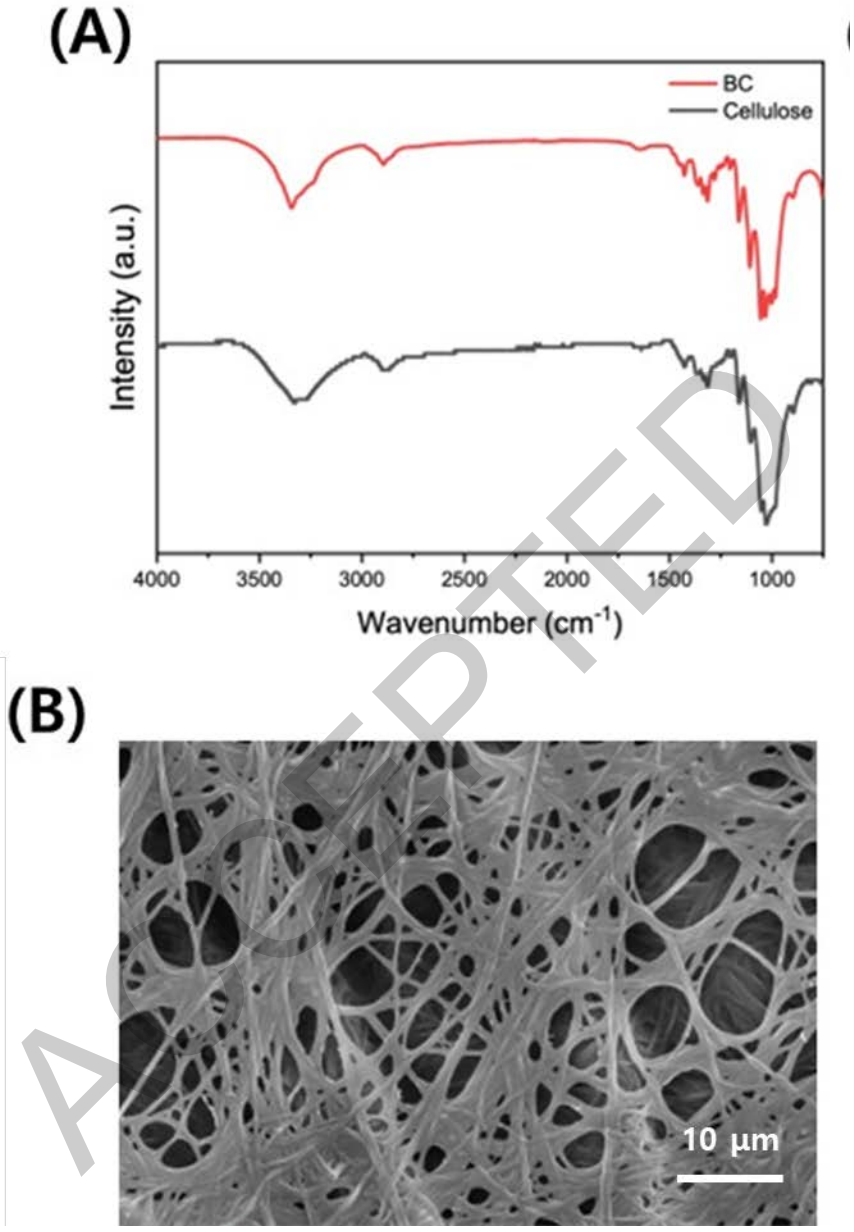

Fig. 5.

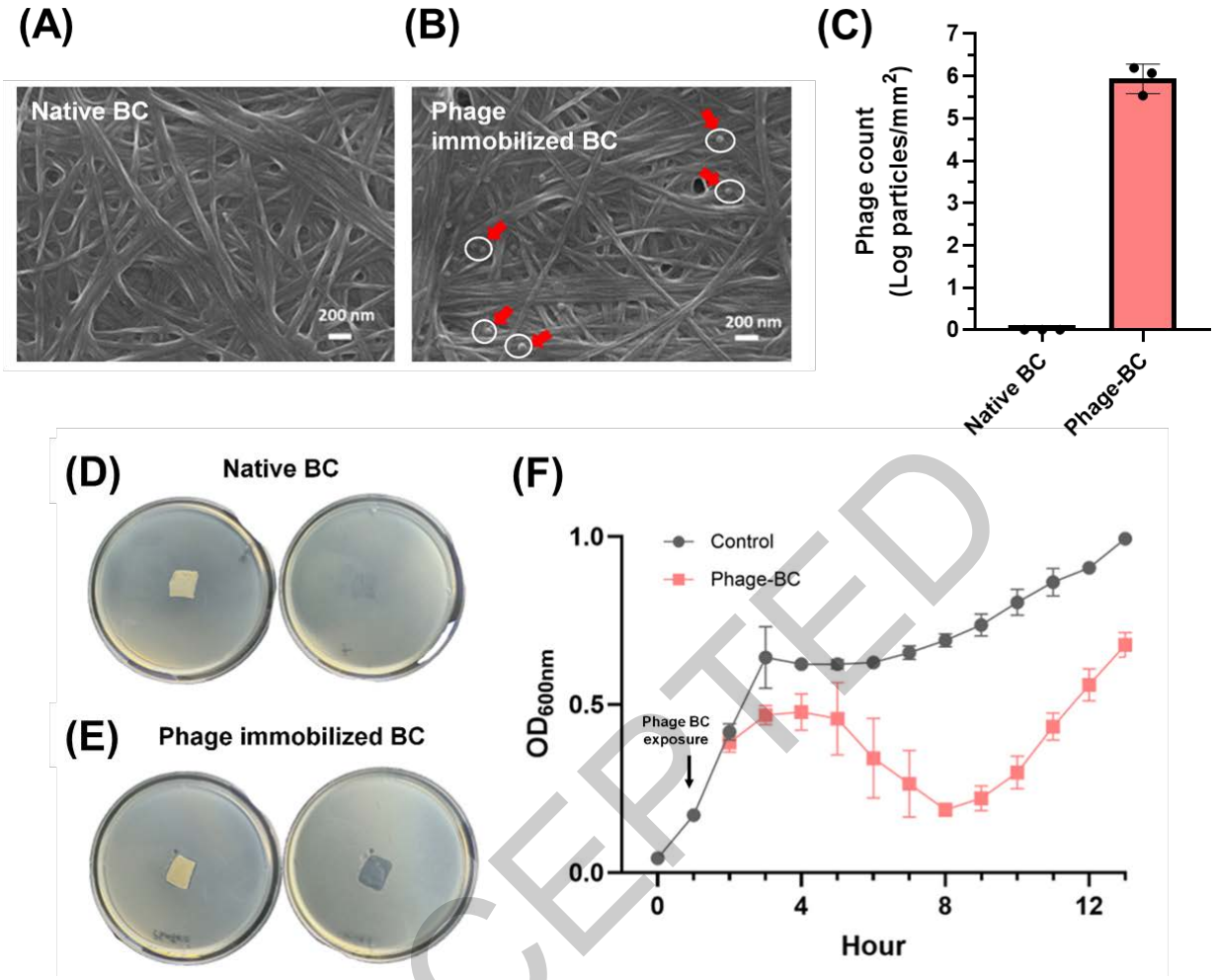

Fig. 6.